Polymer Bulletin
https://doi.org/10.1007/s00289-019-02693-3

ORIGINAL PAPER

Role of CNT/clay hybrid on the mechanical, electrical and transport properties of NBR/NR blends

Saliny Thomas[1] · Jiji Abraham[2] · Soney C. George[1,3] · Sabu Thomas[1,4]

Received: 11 September 2018 / Revised: 4 January 2019 / Accepted: 28 January 2019

Abstract

Hybrid fillers are making a remarkable improvement in the properties of polymeric systems. In the present study, the influence of hybrid of multiwalled carbon nanotube (MWCNT) and nanoclay on the mechanical, electrical and transport properties of nitrile rubber (NBR)/natural rubber (NR) blends has been investigated. Attempts were made to prepare NBR/NR/CNT/nanoclay composites on a two-roll mill and to study various mechanical properties such as tensile strength, tear resistance, abrasion loss and compression set percent. Transport, thermal and electrical properties were also investigated. By virtue of the synergism between MWCNT and nanoclay, the composites exhibited enhancement in the mechanical properties by the immobilization of rubber chains via coupling action between the filler surface and the rubber molecules. The fine and uniform dispersion of both CNT and clay in composite samples supported the observation. The hybrid filler system had a great impact on the thermal and electrical properties of the composites.

✉ Soney C. George
soneygeo@gmail.com

[1] School of Chemical Sciences, Mahatma Gandhi University, Kottayam, Kerala 686560, India

[2] Vimala College (Autonomous), Thrissur, Kerala 680009, India

[3] Centre for Nanoscience and Technology, Department of Basic Sciences, Amal Jyothi College of Engineering, Kanjirappally, Kottayam, Kerala, India

[4] International and Inter University Centre for Nano Science and Nanotechnology, Mahatma Gandhi University, Kottayam, Kerala 686560, India

Graphical abstract

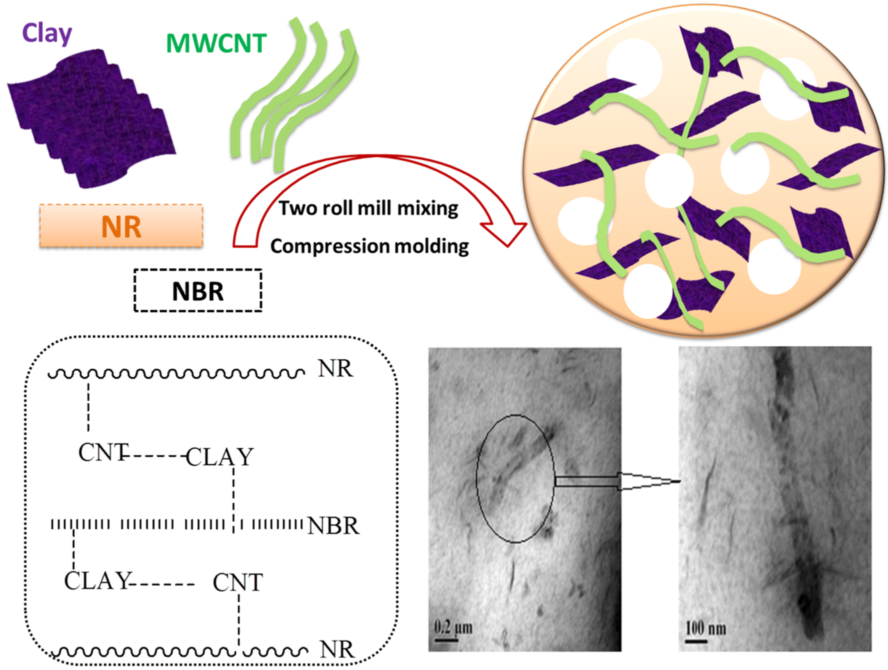

Keywords Hybrid effect · Rubber blends · Immobilization · MWCNT · Clay

Introduction

The incorporation of nanofillers into polymers has been emerged as a good technique for the improvement of the properties of such polymers. This has proved its potential to improve the service properties such as mechanical and thermal and life expectancy, without a considerable increase in density and cost. Reinforcing fillers such as carbon black, silica and resin are found to be increased the strength of vulcanized rubber more than tenfold [1]. The reinforcement of elastomers and the improvement of mechanical properties, to a large extent, are reported to be due to the chemical and physical interactions between the polymer matrix and filler particles [2, 3]. Litvinov et al. [4] studied the adsorption of ethylene propylene diene monomer (EPDM) on carbon black using nuclear magnetic resonance (NMR) technique and reported that reinforcement increased as the EPDM–carbon black interfacial area enhanced.

Hybrid nanomaterials consist of two heterogeneous nanoelementary units with diverse characteristics. These can be used to make a novel class of effective, functional, multidimensional composite nanofillers [5]. Both agglomeration of the nanomaterials and interfacial interaction complications in polymer nanocomposites could be resolved instantaneously by using such functional hybrid nanofillers. Enhanced mechanical performance of Nylon-6 magnetic composites with nanostructured hybrid one-dimensional carbon nanotube/two-dimensional clay nanoplatelets heterostructures was explored by Zhang [6]. Sternstein et al. [7] investigated the reinforcement and concomitant nonlinear viscoelastic behaviour of polymer composites containing hybrid fillers. The results supported the theory already proposed by Sternstein and Zhu [8]. They proposed that the high reinforcement by nanofillers was due to the trapping of entanglements and the consequential effects on mobility of the matrix chain and entropic elasticity. Gao et al. [9] conducted studies on thermal conductivity of epoxy composites using hybrid filler. They observed an enhancement in the thermal conductivity of the epoxy composite containing Al_2O_3/graphene nanohybrid filler compared to the pure epoxy resin. A reduction in the density and an improvement in thermal stability were also observed for the composites containing the nanohybrid fillers. Mousa et al. [10] investigated the cure and mechanical properties of carboxylated nitrile butadiene rubber filled with mixture of nanolayered silicate (NLS) and olive solid waste (OSW). They showed an increase in the glass transition temperature of the composite filled with hybrid filler. The increased storage and loss moduli with reduced mechanical loss factor observed for the composite containing hybrid filler indicated better interaction between the filler–matrix systems.

Rybiński et al. [11] prepared NBR and styrene–butadiene rubber (SBR) composites filled with phthalocyanine–halloysite nanotubes hybrid system and investigated thermal, mechanical flame properties. According to them, the improvement in the mechanical and thermal properties and reduction in flammability of the resultant composites were due to better dispersion of the hybrid filler particles in the matrix. Hemanth et al. [12] prepared thermoplastic copolyester elastomer (TCE) and polyoxymethylene (POM)-filled polytetrafluoroethylene (PTFE) composites, using short glass fibre (SGF) and microfillers such as short carbon fibre (SCF), silicon carbide (SiC) and alumina (Al_2O_3) by melt-mixing method and investigated the mechanical properties.

Huang et al. [13] studied the synergistic effect of nano- and micro-$BaTiO_3$ on the electrical and mechanical properties of ethylene vinyl acetate (EVA) composites. From the morphological analysis, they could observe that there was no voiding at the polymer–filler interphase and the hybrid filler system improved the interfacial adhesion with EVA. The hybrid filler system was not only able to reduce the interfacial tension but could also prevent the coalescence of the nanoparticles during processing. Praveen et al. reported that styrene–butadiene rubber (SBR) composites containing 10 phr nanoclay and 20 phr carbon black (CB) exhibited high tensile strength as 21.6 MPa by synergistic action between the fillers and the rubber matrix [14]. Reports from [15] also showed that CB improved CNT dispersion in styrene–butadiene copolymer matrix. Carbon nanotube (CNT) is interacted with carbon black (CB) surface, thereby enhancing the electrical and mechanical properties of the composite.

Since no systematic studies are reported on the evaluation of physico-mechanical, electrical, thermal and transport properties of NBR/NR blend filled with

CNT/nanoclay, attempts were made to prepare NBR/NR/CNT/nanoclay composites on a two-roll mill and study various mechanical properties along with electrical, thermal and transport properties. The composites exhibited improvement in the properties.

Materials and methods

Materials

Natural rubber (poly-cis-2-methyl butadiene) ISNR-5 grade supplied by Rubber Research Institute of India, Kottayam, was used in the present study. Acrylonitrile butadiene rubber (NBR) under the trade name N-684, with ACN%—33, Mooney viscosity 35–44 units at 100 °C was supplied by Chemigum. Rubber chemicals such as zinc oxide, sulphur and stearic acid were of commercial grade and were supplied by Merck India Pvt Ltd. Vulcanization accelerators such as *N*-cyclohexyl benzthiazyl sulfenamide (CBS), tetramethyl thiuramdisulfide (TMTD) and antioxidant 2.4-trimethyl-1.2-dihydroquinoline (TDQ) were also supplied by Merck India Pvt Ltd. Multiwalled carbon nanotube (MWCNT) of aspect ratio 140 was supplied by Nanocyl, Belgium. Nanoclay (Cloisite 93A) was supplied by Southern Clay Products, USA. The modifier concentration and specific gravity of the nanoclay are 90 cmol kg^{-1} and 1.88 g mL^{-1}, respectively.

Compounding of rubber

Compounding of rubber was done on a laboratory size two-roll mixing mill (15.3 × 30.5 cm, Indian Expeller) as per ASTM designation D3182-89, first by masticating NR for 10 min for lowering its viscosity and then mixing other ingredients in the order as zinc oxide, stearic acid, accelerators, filler and sulphur. Mixing was continued for a further 3 min, and the batch was homogenized by passing it in single direction to ensure the orientation of chains and to preserve mill direction before moulding. The total mixing time and roll temperature were kept constant throughout the study.

Vulcanization

Vulcanization of the rubber compounds was done in an electrically heated laboratory-type hydraulic press (Indian Expeller) at 150 °C at a pressure of 120 kg cm^{-2} up to the optimum cure time in respective moulds. The moulded samples were kept in a cold and dark place for 24 h and then used for various measurements. The membranes of 1.5 mm thickness were used for permeation studies. NR/NBR/organoclay/CNT hybrid composites were prepared as per the recipe shown in Table 1.

Table 1 NR/NBR/MWCNT/organoclay formulations in phr

Sample	NR	NBR	CNT	Clay	Zinc oxide	Stearic acid	TDQ	CBS	Sulphur
$NRCT_1$	100	0	4	0	5	2	1	1	2.5
$NRCT_2$	100	0	4	1	5	2	1	1	2.5
$NRCT_3$	100	0	4	2	5	2	1	1	2.5
$NRCT_4$	100	0	0	4	5	2	1	1	2.5
$NRCT_5$	100	0	1	4	5	2	1	1	2.5
$NRCT_6$	100	0	2	4	5	2	1	1	2.5
$NBCT_1$	0	100	4	0	5	2	1	1	2.5
$NBCT_2$	0	100	4	1	5	2	1	1	2.5
$NBCT_3$	0	100	4	2	5	2	1	1	2.5
$NBCT_4$	0	100	0	4	5	2	1	1	2.5
$NBCT_5$	0	100	1	4	5	2	1	1	2.5
$NBCT_6$	0	100	2	4	5	2	1	1	2.5
$BLCT_1$	70	30	4	0	5	2	1	1	2.5
$BLCT_2$	70	30	4	1	5	2	1	1	2.5
$BLCT_3$	70	30	4	2	5	2	1	1	2.5
$BLCT_4$	70	30	0	4	5	2	1	1	2.5
$BLCT_5$	70	30	1	4	5	2	1	1	2.5
$BLCT_6$	70	30	2	4	5	2	1	1	2.5

Parts per hundred parts of rubber

Characterization techniques

Cure characteristics

The cure behaviour of rubber compound was measured using automated Goettfert elastograph; model Vario 67.98 (German) at 150 °C. It is a rotor less rotational shear vulcameter with a chamber for placing the rubber compound. All the cure properties were directly obtained using software.

The data obtained from the instrument are:

(i) Minimum torque (M_L): This is the torque attained by the mix at the test temperature before the onset of cure.
(ii) Maximum torque (M_H): This is the torque recorded after the completion of cure process.
(iii) Scorch time (ts_2): This is the time taken for two-unit rise of torque above minimum torque (time required for 10% vulcanization).
(iv) Optimum cure time (t_{90}): This is the time taken for attaining 90% of the maximum torque (90% vulcanization) and can be calculated using Eq. 1:

$$t_{90} = 0.9\left(M_H - M_L\right) + M_L \tag{1}$$

(v) Cure rate index (CRI): this is calculated as:

$$\mathrm{CRI} = 100/\left(t_{90} - \mathrm{ts}_2\right) \tag{2}$$

Mechanical properties

X-ray diffraction analysis (XRD) X-ray diffraction patterns of the samples were taken using Ni-filtered CuKα radiation at a generator voltage of 60 keV and a generator current of 40 mA and wavelength of 0.154 nm at room temperature. The samples were scanned in the range of 10°.

Tensile properties Tensile properties of the vulcanizates were measured on a Universal Testing Machine, Instron Corporation, series IX model 1034, using a crosshead speed of 500 mm/min as per ASTM D412-2016, using dumb-bell-shaped vulcanizate. Five samples of each vulcanized sheet were used for the measurement. The values were directly obtained from the instrument. Tensile strength and modulus were reported in MPa and elongation at break (EB) in percentage.

Tear resistance The test samples were cut from the vulcanized sheets parallel to the grain direction. The test pieces were mounted on a Universal Testing Machine, Instron Corporation, series IX model 1034, using a crosshead speed of 500 mm/min as per ASTM method D 624-2007. Five samples of each vulcanized sheet were used for the measurement. Tear resistance was directly obtained in N/mm.

Compression set Compression set was determined as per ASTM D395-2008 (method B) using the apparatus manufactured by Prolific Engineers India Ltd. The moulded samples (1.25 cm thick and 2.8 cm diameter) compressed to constant deflection (25%) were kept for 22 h at 27 °C. The samples were taken out, and after keeping for 30 min, the final thickness was measured. The compression set % is calculated using Eq. 3. Three samples of each mix are used for compression set determination.

$$\text{Compression set}\,\% = \frac{(t_0 - t_1) \times 100}{t_0 - t_\mathrm{s}} \tag{3}$$

where t_0 and t_1 are the initial and final thicknesses of the specimen and t_s is the thickness of the space bar used.

Abrasion loss Abrasion loss was determined using DIN abrader (DIN 5963). Moulded sample having a diameter of 6 ± 0.2 mm and a thickness of 6 mm was inserted into the sample holder so that 2 mm of the sample remained exposed and allowed to move across the surface of an abrasive sheet mounted on a rotating drum. Weight of the test specimen was noted before and after the test. The difference in weight, reported as the weight loss, was converted into volume loss by dividing the weight loss with the density of the specimen. Three moulded samples of each mix were used for the determination of abrasion loss, and the final result was expressed as the average of these results.

Determination of total crosslink density Circular samples of approximately 1 cm diameter and 0.2 cm thickness were punched out from the central portions of the vulcanized sheet and weighed. These samples were allowed to swell in toluene at room temperature up to equilibrium swelling. The swollen samples were taken out and weighed again after blotting out the solvent from the surface of the samples using blotting paper. The solvent was removed in vacuum and the weight of the de-swollen samples was again determined and the crosslink density υ is calculated using Eq. (4)

$$\text{Crosslink density } \upsilon = \frac{1}{2M_c} \tag{4}$$

where M_c is the molecular weight of the polymer between crosslinks and is calculated using Eq. (5)

$$M_c = \frac{\rho_p V_s V_{rf}^{\frac{1}{3}}}{\ln\left\{1 - V_{rf}\right\} + V_{rf} + \chi V_{rf}^2} \tag{5}$$

V_s is the molar volume of the solvent (toluene $V_s = 106.2$ cm^3 mol^{-1}), ρ_p is the density of the polymer, χ is the interaction parameter, V_{rf} is the volume fraction of rubber in the solvent–swollen filled sample. V_{rf} is given by the equation of Ellis and Welding 6.

$$V_{rf} = \frac{(d - fw)/\rho_p}{d - fw/\rho_p + A_s/\rho_s} \tag{6}$$

where d is the de-swollen weight, f is the weight fraction of the filler in the rubber vulcanizates, w is the initial weight of the sample, ρ_p is the density of the polymer, ρ_s is the density of the solvent (toluene = 0.886 g/cm^3) and A_s is the amount of the solvent absorbed.

Thermodynamic parameters (ΔG and ΔS) The change in elastic Gibb's free energy (ΔG) is determined from the Flory–Huggins Eq. (7) as given below:

$$G = RT\left[\ln\left(1 - v_{rf}\right) + v_{rf} + \chi v_{rf^2}\right] \tag{7}$$

From the statistical theory of rubber elasticity, the conformational entropy (ΔS) is calculated using Eq. (8):

$$\Delta S = -\frac{\Delta G}{T} \tag{8}$$

Results and discussion

XRD

Figure 1 shows the XRD pattern of nanoclay, CNT and hybrid nanocomposites. Nanoclay (Cloisite 93A) shows an intense peak at 3.86°. But the absence of sharp peak at 3.86° in the XRD of BLCT2 and BLCT5 reveals the dispersion of nanoclay in the polymer matrix. MWCNT shows sharp peak at 25°. The reduction in intensity and also the shift from the expected angle 25°–20° in the case of BLCT2 and BLCT5 should be due to dispersion of CNT in the polymer matrix. The reduction of peak intensity for CNT in the case of BLCT5 reveals that the dispersion of CNT is more effective in BLCT5 than that in BLCT2.

Cure properties

Cure properties of NR, NBR and their blend vulcanizates filled with CNT and clay as hybrid fillers are shown in Table 2. Compared to gum vulcanizates, the M_L and M_H of CNT-filled NR, NBR and their blend vulcanizates were decreased. Also, the addition of clay, either itself or along with CNT, decreases the M_L and M_H values. Under high shear, the rubber chains were entered into the organoclay galleries and their domain size is much reduced. Along this, the presence of CNT provides maximum dispersion of clay layers. Consequently, the torque values decreased. Also, the clay/CNT hybrid fillers reduced the values of ts_2 and t_{90} and increases CRI values than that of gum vulcanizates. In all matrix systems (NR, NBR and NR/NBR blend), 4 phr clay/2 phr CNT combinations show enhanced cure properties. Ammonium molecules in organoclay galleries play an important role in sulphur vulcanization of rubber nanocomposites. In hybrid filler system, both clay and CNT help the dispersion of one another and thus avoid the agglomeration in some extent. The nanotubes that entered into the organoclay galleries help the intercalation of clay layers.

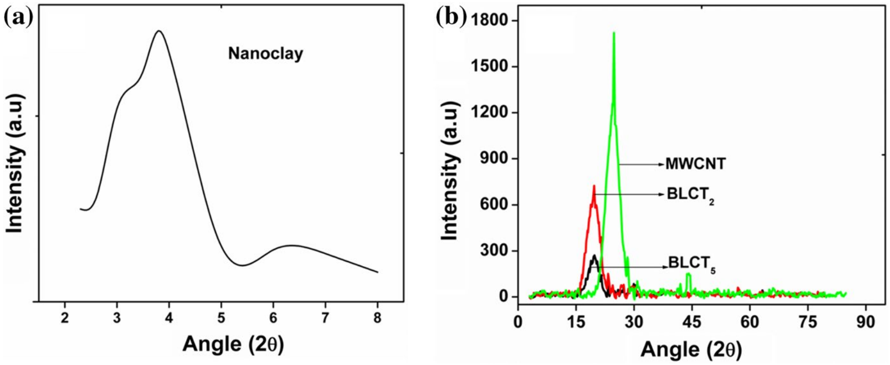

Fig. 1 XRD pattern of nanoclay, CNT and nanocomposites

Table 2 Cure properties of 70NR/30NBR/CNT/clay nanocomposites

Sample	Minimum torque, M_L (dNm)	Maximum torque, M_H (dNm)	Optimum cure time, t_{90} (min)	Scorch time, ts_2 (min)	Cure rate index, CRI
$NRCT_1$	2.726 ± 0.022	52.472 ± 0.404	10.164 ± 0.153	2.417 ± 0.313	12.914 ± 0.057
$NRCT_2$	2.663 ± 0.034	51.443 ± 0.241	9.851 ± 0.241	2.352 ± 0.164	13.332 ± 0.051
$NRCT_3$	2.654 ± 0.018	50.194 ± 0.135	9.725 ± 0.172	2.274 ± 0.211	13.426 ± 0.031
$NRCT_4$	2.664 ± 0.023	52.303 ± 0.091	9.926 ± 0.265	2.381 ± 0.243	13.253 ± 0.139
$NRCT_5$	2.643 ± 0.013	51.291 ± 0.511	9.874 ± 0.164	2.361 ± 0.213	13.317 ± 0.014
$NRCT_6$	2.631 ± 0.015	50.052 ± 0.462	9.813 ± 0.172	2.355 ± 0.162	13.406 ± 0.011
$NBCT_1$	4.174 ± 0.031	52.161 ± 0.272	10.421 ± 0.197	2.421 ± 0.068	12.500 ± 0.153
$NBCT_2$	4.125 ± 0.050	51.815 ± 0.214	10.324 ± 0.081	2.344 ± 0.012	12.546 ± 0.184
$NBCT_3$	3.971 ± 0.041	51.277 ± 0.187	10.240 ± 0.102	2.267 ± 0.041	12.552 ± 0.076
$NBCT_4$	4.116 ± 0.034	51.831 ± 0.421	10.348 ± 0.411	2.335 ± 0.137	12.479 ± 0.422
$NBCT_5$	4.095 ± 0.015	51.673 ± 0.235	10.246 ± 0.216	2.313 ± 0.091	12.618 ± 0.431
$NBCT_6$	3.923 ± 0.27	51.214 ± 0.411	10.183 ± 0.208	2.268 ± 0.073	12.624 ± 0.094
$BLCT_1$	2.917 ± 0.017	52.910 ± 0.251	10.263 ± 0.055	2.421 ± 0.275	12.751 ± 0.079
$BLCT_2$	2.853 ± 0.124	52.583 ± 0.315	10.136 ± 0.104	2.376 ± 0.421	12.894 ± 0.024
$BLCT_3$	2.830 ± 0.009	52.371 ± 0.254	10.025 ± 0.026	2.323 ± 0.233	12.996 ± 0.195
$BLCT_4$	2.837 ± 0.117	52.273 ± 0.281	10.182 ± 0.342	2.407 ± 0.419	12.861 ± 0.143
$BLCT_5$	2.822 ± 0.172	52.155 ± 0.131	10.131 ± 0.008	2.374 ± 0.271	12.882 ± 0.026
$BLCT_6$	2.791 ± 0.031	52.094 ± 0.246	9.838 ± 0.134	2.322 ± 0.264	13.315 ± 0.007

Mechanical properties

Tensile test was used in order to study the effect of double-phase filler on the mechanical behaviour of NR, NBR and their blend vulcanizates. All the results are shown in Table 3. The addition of organoclay as well as CNT to NR, NBR and their blend improved the tensile strength, tear strength and modulus of these nanocomposites. But, the most important findings from this study are that the addition of double-phase filler, i.e. organoclay and CNT, improves the mechanical properties of the nanocomposites than the single-phased ones. The filler–filler interaction can be reduced and thus induced a fine and efficient dispersion of both the fillers. The synergism between CNT and clay occurs due to possibility of bonding between the functional groups of clay and CNT [16]. Thus, CNT–clay units entrapped between the rubber chains will bridge the NR and NBR chains, leading to the immobilization of the polymer chains [17, 18].

The effective dispersion of organoclay and CNT led to the high mechanical efficiency of double-phase filler nanocomposites. One intercalated clay particle can interrupt the CNT–CNT network by occupying a position in between them. Also, a single carbon nanotube can be placed between the organoclay galleries. This could reduce the overall filler–filler network.

The results of the compression set for the NR/NBR samples containing double-phase fillers (nanoclay and CNT) are shown in Table 3. From these results, it is

Table 3 Mechanical properties of 70NR/30NBR/CNT/clay nanocomposites

Samples	Tensile strength (MPa)	100% modulus (MPa)	Tear strength (N/mm)	Abrasion loss (mm^3)	Compression set (%)	Crosslink density × 10^4 (gmol/cc)	ΔG (J/mol)	ΔS (J/mol/K)
NRCT1	11.74 ± 0.14	1.28 ± 0.003	48.03 ± 3.4	286 ± 4	1.59 ± 0.04	1.09 ± 0.012	−33.40 ± 0.74	0.110 ± 0.002
NRCT2	13.82 ± 0.13	1.36 ± 0.002	50.31 ± 1.3	275 ± 2	1.54 ± 0.02	1.13 ± 0.007	−38.76 ± 0.24	0.129 ± 0.001
NRCT3	15.02 ± 0.16	1.39 ± 0.002	52.73 ± 0.9	270 ± 4	1.41 ± 0.04	1.18 ± 0.002	−42.27 ± 0.13	0.141 ± 0.001
NRCT4	11.95 ± 0.13	1.30 ± 0.002	49.24 ± 3.7	287 ± 5	1.62 ± 0.02	1.12 ± 0.001	−35.96 ± 0.71	0.119 ± 0.002
NRCT5	14.51 ± 0.15	1.38 ± 0.003	50.80 ± 1.5	281 ± 2	1.59 ± 0.02	1.14 ± 0.006	−40.28 ± 0.27	0.134 ± 0.001
NRCT6	15.92 ± 0.17	1.41 ± 0.003	53.41 ± 2.4	272 ± 4	1.58 ± 0.01	1.21 ± 0.004	−43.57 ± 0.42	0.145 ± 0.002
NBCT1	3.96 ± 0.23	1.48 ± 0.013	23.81 ± 2.4	180 ± 3	2.98 ± 0.11	1.40 ± 0.004	−61.87 ± 0.21	0.206 ± 0.001
NBCT2	5.07 ± 0.19	1.52 ± 0.005	25.3 ± 2.1	179 ± 5	2.94 ± 0.01	1.42 ± 0.002	−65.12 ± 0.27	0.217 ± 0.001
NBCT3	6.22 ± 0.21	1.57 ± 0.002	26.7 ± 1.4	176 ± 4	2.94 ± 0.02	1.45 ± 0.005	−69.45 ± 0.34	0.232 ± 0.001
NBCT4	4.15 ± 0.47	1.45 ± 0.004	24.01 ± 1.8	179 ± 4	179 ± 0.01	1.42 ± 0.003	−64.82 ± 0.28	0.216 ± 0.001
NBCT5	5.12 ± 0.13	1.47 ± 0.003	26.26 ± 1.8	170 ± 2	3.12 ± 0.02	1.43 ± 0.002	−67.32 ± 0.13	0.224 ± 0.001
NBCT6	6.31 ± 0.24	1.51 ± 0.002	28.45 ± 1.3	168 ± 4	3.09 ± 0.01	1.45 ± 0.004	−68.93 ± 0.17	0.230 ± 0.001
BLCT1	10.38 ± 0.25	1.08 ± 0.005	42.38 ± 2.5	283 ± 4	2.21 ± 0.03	1.20 ± 0.002	−41.0 ± 0.96	0.136 ± 0.003
BLCT2	12.78 ± 0.18	1.13 ± 0.002	44.18 ± 2.6	266 ± 5	2.18 ± 0.02	1.22 ± 0.001	−46.37 ± 0.16	0.154 ± 0.001
BLCT3	13.14 ± 0.23	1.17 ± 0.003	45.53 ± 1.8	261 ± 3	2.14 ± 0.01	1.25 ± 0.007	−52.81 ± 0.54	0.176 ± 0.002
BLCT4	10.5 ± 0.18	1.09 ± 0.002	43.6 ± 3.1	275 ± 5	2.18 ± 0.02	1.23 ± 0.002	−43.40 ± 0.29	0.144 ± 0.001
BLCT5	12.63 ± 0.22	1.14 ± 0.003	45.84 ± 1.3	267 ± 3	2.16 ± 0.02	1.26 ± 0010	−49.15 ± 0.34	0.163 ± 0.001
BLCT6	13.28 ± 0.27	1.19 ± 0.004	47.19 ± 2.2	265 ± 4	2.12 ± 0.03	1.28 ± 0.002	−53.73 ± 0.42	0.179 ± 0.001

revealed that the insertion of the double-phase filler reduces the deformation sustained by the elastomer than that of single fillers. This might be due to the fact that the polymer chains embedded within the CNTs and nanoclay layers prevent them to be abraded out from the surface. Both CNTs and nanoclay provided a coupling action between the filler surface and the rubber molecules, causing a reduction in the abrasion loss, compared with the blend composite containing single filler like clay alone or CNT alone. The synergism between CNT and clay occurs due to the possibility of bonding between the functional groups of clay and CNT as shown in Fig. 2.

The CNTs embedded in the rubber matrix are much harder than the rubber, and this rigid phase insulated the rubber against abrasion. Bhattacharya et al. reported that synergistic effect of carbon black in the presence of nanofibre and nanoclay reduces the abrasion loss of natural rubber nanocomposites [19]. The effect of fillers on the crosslink density [CD] of the polymer matrix is given in Table 3. The vulcanizates that contain double-phase filler shows enhanced crosslink density as compared to single-phase vulcanizates. The increase in crosslink density can be attributed to the large contact area between the clay/CNT and the elastomer matrix in the NR/NBR composite. Thus, CNT–clay units entrapped between the rubber chains immobilize the polymer chains.

Thermodynamic parameters ΔG and ΔS are calculated using Eqs. (7) and (8), respectively. These parameters are given in Table 3. The more negative change in free energy values shows better compatibility between the filler and the matrix [20]. On increasing the filler dosage, the interfacial area gets increased up to a certain level, due to the decrease in size of dispersed phase by the influence of nanoclay. In this study, ΔG values are found to be more negative as the concentration of hybrid filler increases. In the case of blend, maximum $-\Delta G$ value was shown by the mix containing 4 phr clay and 2 phr CNT (BLCT$_6$). It revealed that in the immiscible NR/NBR blend system the hybrid filler system acted as a compatibilizing agent.

ΔS values are also found to be increasing as the concentration of the hybrid filler increases. In the case of blend, maximum ΔS value was shown by the

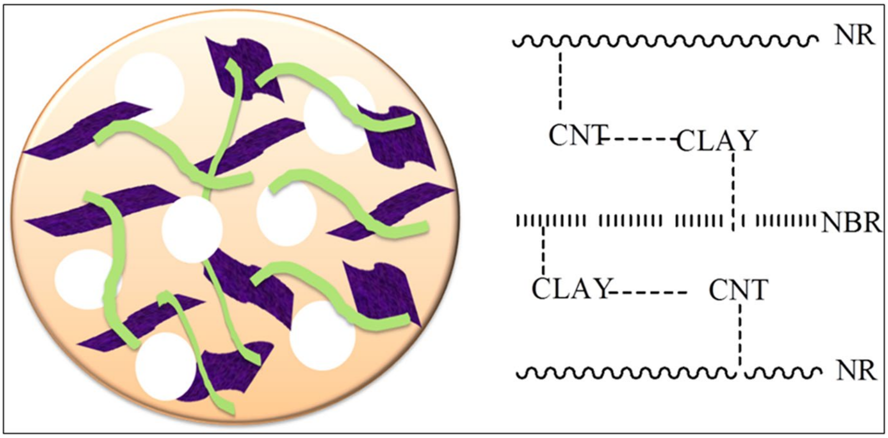

Fig. 2 Schematic representation of CNT/clay bridges between NR and NBR chains

mix containing 4 phr clay and 2 phr CNT. In the case of blend, maximum ΔS value was shown by the mix containing 4 phr clay and 2 phr CNT ($BLCT_6$). The increase in entropy reveals the disorder of the system, and hence, it indicates the enhanced compatibility. This is achieved by the synergism between the fillers helping to form additional bridges between the two polymer phases.

Swelling properties

The swelling of polymer is affected by solvent transport [21]. As free volume increases, swelling of the rubber composite thereby increases the chain mobility, which facilitates the transport of solvent molecules [22]. The presence of fillers reduced the free space for solvent molecules in the intercalated structure of the nanocomposites.

This shows the strong interaction between the filler and the matrix, which limits the diffusivity of solvent within the entangled polymer matrix. Figure 3 shows the nature of toluene uptake by nanocomposites. The Qt values of the hybrid nanocomposites were lower than those of the nanocomposites, which contain only one type of filler. Solvent resistance is greater for the composite containing hybrid filler system than that containing single filler, because the use of high concentration of single filler leads to agglomeration. As compared to CNT, nanoclay is more intercalated in NR/NBR matrix. The use of nanoclay as the major filler is

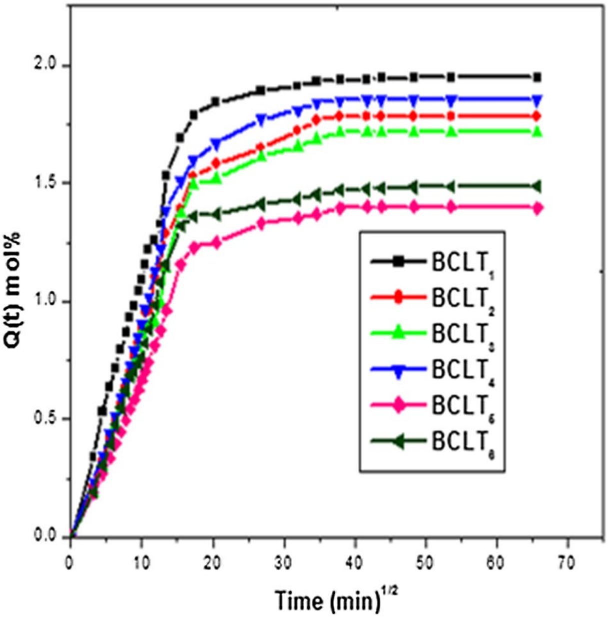

Fig. 3 Swelling characteristics of NR/NBR blend filled with CNT/clay filler system

more effective. So $BLCT_5$ and $BLCT_6$ have more solvent resistance than $BLCT_2$ and $BCLT_3$. Also, the increase in concentration of CNT leads to agglomeration.

Microscopic analysis (transmission electron microscopy)

TEM images of NR/NBR/CNT/clay nanocomposites are shown in Fig. 4. The state of dispersion of fillers in the matrix, which significantly affects the electrical and mechanical properties of the material, is evident from the TEM analysis of the composites. In Fig. 4a, b, it is revealed that the dispersion of CNT is well in $BLCT_2$ as compared to $BLCT_3$ sample. The fine and uniform dispersion of both CNT and clay in $BLCT_5$ and $BLCT_6$ samples can be seen in Fig. 4c, d. It is also clear that the distance between the CNTs in the matrix is wide and the clay particle plays an important role to make them well oriented with little interface interaction between them. The figures also indicate that the orientation of the CNTs and clay particles play a very important role in the stress and strain of the matrix. Both CNT and clay help the dispersion of one another by way of synergism and thus avoid the agglomeration to some extent.

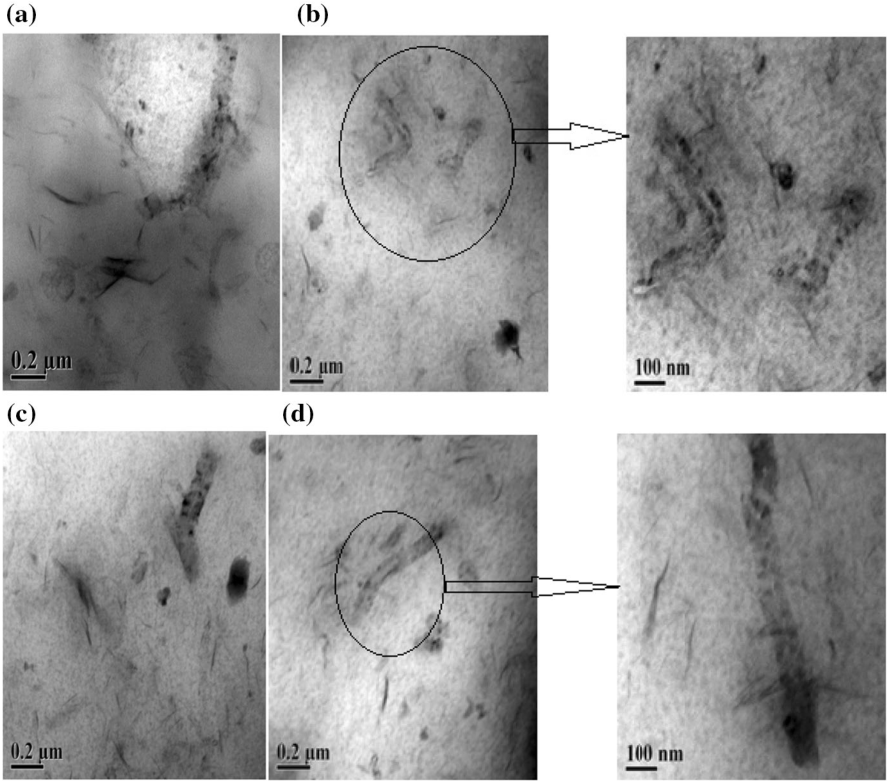

Fig. 4 TEM images of CNT-/clay-filled NBR/NR vulcanizates

Electrical properties

The conduction of the CNT/clay hybrid-filled composites is better explained using percolation theory and interfacial polarization mechanism. Interfaces can be formed between the non-conducting rubber matrix and the carbon nanotubes. The large π orbitals of the MWCNTs provided domains for nomadic electrons. These can be oriented under the electric field, resulting in interfacial polarization [23]. The particular arrangements of conductive elements in the network help the free movement of electron through the polymer matrix. From the number of results available in the literature, it is now evident that very small quantities of carbon nanotubes are required to get relatively high values of electrical conductivity. Figure 4 shows that the conductivity of NR/NBR blends increases with the filler concentration. It was reported that the electrical properties depend upon the filler concentration, polymer matrix and filler–matrix interaction [24]. The conductivity of all the vulcanizates showed an increase with frequency (Fig. 5). This can be due to the increase in segmental mobility of the polymer matrix at higher frequency level.

Conclusions

A kind of synergism helps the finer dispersion of both CNT and clay in the rubber matrix. The TEM images show that the distance between the CNTs is wide and the clay particles help CNTs keep well oriented. The CNT/clay bridges can keep the NR/NBR chains bound. This has led to the fine and uniform dispersion of the hybrid filler. The double-phase filler system has caused an enhancement in the crosslink density and the mechanical properties such as tensile strength and tears resistance,

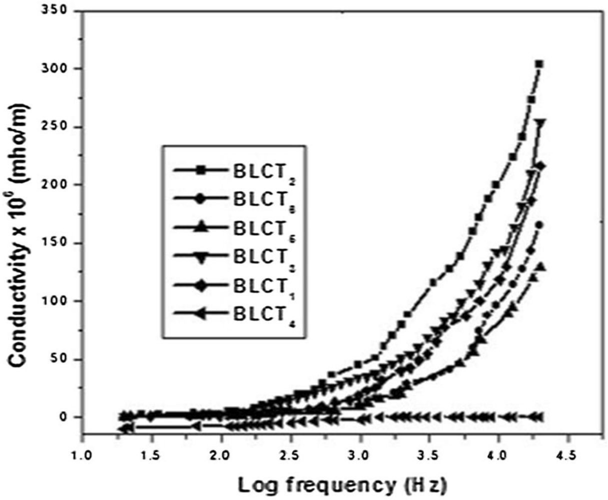

Fig. 5 Conductivity versus log frequency plots for NBR/NR blends filled with hybrid filler

which is attributed to the large contact area between clay and CNT. The improved filler–polymer matrix interaction has enhanced the electrical properties also.

References

1. Khan MS, Lehmann D, Heinrich G (2008) Modification of PTFE nanopowder by controlled electron beam irradiation: a useful approach for the development of PTFE coupled EPDM compounds. Express Polym Lett 2:284–293
2. Wolff S, Wang MJ (1992) Filler—elastomer interactions. Part IV. The effect of the surface energies of fillers on elastomer reinforcement. Rubber Chem Technol 65(2):329–342
3. Fröhlich J, Niedermeier W, Luginsland HD (2005) The effect of filler–filler and filler–elastomer interaction on rubber reinforcement. Compos A Appl Sci Manuf 36(4):449–460
4. Litvinov VM, Steeman PAM (1999) EPDM–carbon black interactions and the reinforcement mechanisms, as studied by low-resolution 1H NMR. Macromolecules 32(25):8476–8490
5. Sanchez C, Soler-Illia GDA, Ribot F, Lalot T, Mayer CR, Cabuil V (2001) Designed hybrid organic–inorganic nanocomposites from functional nanobuilding blocks. Chem Mater 13(10):3061–3083
6. Zhang C, Tjiu WW, Liu T, Lui WY, Phang IY, Zhang WD (2011) Dramatically enhanced mechanical performance of nylon-6 magnetic composites with nanostructured hybrid one-dimensional carbon nanotube—two-dimensional clay nanoplatelet heterostructures. J Phys Chem B 115(13):3392–3399
7. Sternstein SS, Ramorino G, Jiang B, Zhu AJ (2005) Reinforcement and nonlinear viscoelasticity of polymer melts containing mixtures of nanofillers. Rubber Chem Technol 78(2):258–270
8. Sternstein SS, Zhu AJ (2002) Reinforcement mechanism of nanofilled polymer melts as elucidated by nonlinear viscoelastic behavior. Macromolecules 35(19):7262–7273
9. Gao Z, Zhao L (2015) Effect of nano-fillers on the thermal conductivity of epoxy composites with micro-Al2O3 particles. Mater Des 1980–2015(66):176–182
10. Mousa A, Heinrich G, Wagenknecht U (2013) The application of solid olive waste as reinforcement in carboxylated nitrile butadiene rubber/organo nano layered silicates composites. J Solid Waste Technol Manag 39(3):197–203
11. Rybiński P, Pająk A, Janowska G, Jóźwiak M (2015) Effect of hybrid filler (HNTs-phthalocyanine) on the thermal properties and flammability of diene rubber. J Appl Polym Sci 132(40):1–20
12. Hemanth R, Sekar M, Suresha B (2014) Effects of fibers and fillers on mechanical properties of thermoplastic composites. Indian J Adv Chem Sci 2:28–35
13. Huang X, Xie L, Hu Z, Jiang P (2011) Influence of $BaTiO_3$ nanoparticles on dielectric, thermophysical and mechanical properties of ethylene-vinyl acetate elastomer/$BaTiO_3$ microcomposites. IEEE Trans Dielectr Electr Insul 18(2):375–383
14. Praveen S, Chattopadhyay PK, Albert P, Dalvi VG, Chakraborty BC, Chattopadhyay S (2009) Synergistic effect of carbon black and nanoclay fillers in styrene butadiene rubber matrix: development of dual structure. Compos A Appl Sci Manuf 40(3):309–316
15. Bokobza L, Rahmani M, Belin C, Bruneel JL, El Bounia NE (2008) Blends of carbon blacks and multiwall carbon nanotubes as reinforcing fillers for hydrocarbon rubbers. J Polym Sci Part B Polym Phys 46(18):1939–1951
16. Song SH (2018) The effect of clay/multiwall carbon nanotube hybrid fillers on the properties of elastomer nanocomposites. Int J Polym Sci 2018:5295973-1–5295973-8. https://doi.org/10.1155/2018/5295973
17. Pradhan B, Roy S, Srivastava SK, Saxena A (2015) Synergistic effect of carbon nanotubes and clay platelets in reinforcing properties of silicone rubber nanocomposites. J Appl Polym Sci 132(15):1–11
18. Abraham J, Thomas J, Kalarikkal N, George SC, Thomas S (2018) Static and dynamic mechanical characteristics of ionic liquid modified MWCNT-SBR composites: theoretical perspectives for the nanoscale reinforcement mechanism. J Phys Chem B 122(4):1525–1536
19. Bhattacharya M, Bhowmick AK (2010) Synergy in carbon black-filled natural rubber nanocomposites. Part I: mechanical, dynamic mechanical properties, and morphology. J Mater Sci 45(22):6126–6138

20. Abraham J, Maria HJ, George SC, Kalarikkal N, Thomas S (2015) Transport characteristics of organic solvents through carbon nanotube filled styrene butadiene rubber nanocomposites: the influence of rubber–filler interaction, the degree of reinforcement and morphology. Phys Chem Chem Phys 17(17):11217–11228
21. Abraham J, Muraleedharan K, Radhesh Kumar C, Thomas S, George SC (2017) Solvent transport characteristics of thermoplastic elastomer blends based on nylon and NBR. Polym Eng Sci 57(2):231–236
22. Thomas S, Thomas S, Abraham J, George SC, Thomas S (2018) Investigation of the mechanical, thermal and transport properties of NR/NBR blends: impact of organoclay content. J Polym Res 25(8):165
23. Abraham J, Kailas L, Kalarikkal N, George SC, Thomas S (2016) Developing highly conducting and mechanically durable styrene butadiene rubber composites with tailored microstructural properties by a green approach using ionic liquid modified MWCNTs. RSC Adv 6(39):32493–32504
24. Abraham J, Xavier P, Bose S, George SC, Kalarikkal N, Thomas S (2017) Investigation into dielectric behaviour and electromagnetic interference shielding effectiveness of conducting styrene butadiene rubber composites containing ionic liquid modified MWCNT. Polymer 112:102–115